

Velocity distribution $f(v_{\parallel}, v_{\perp})$ at injection site

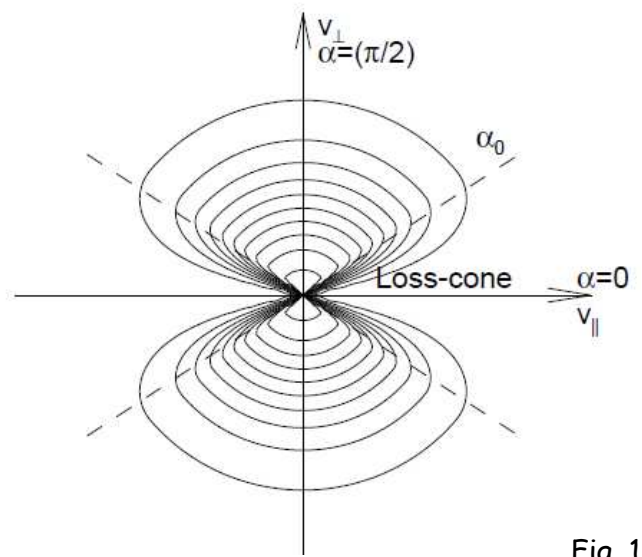
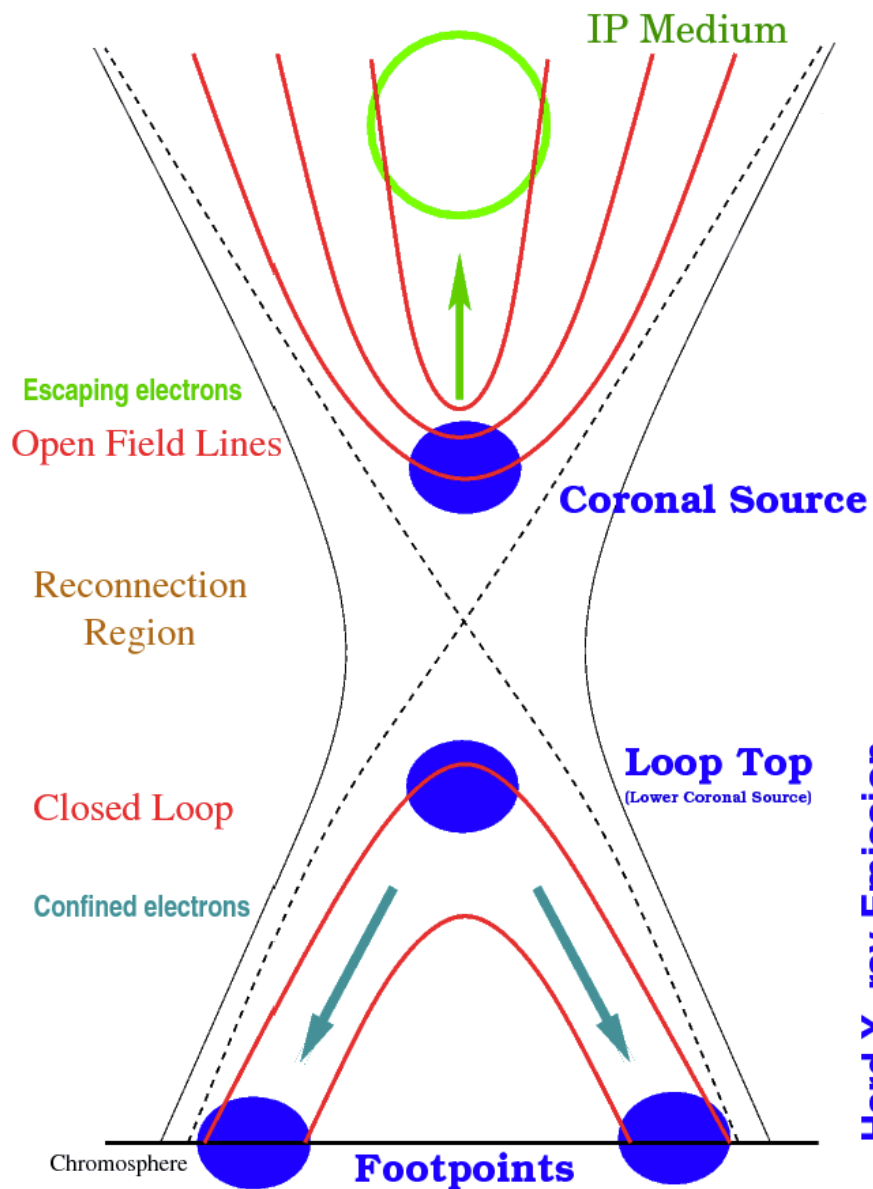
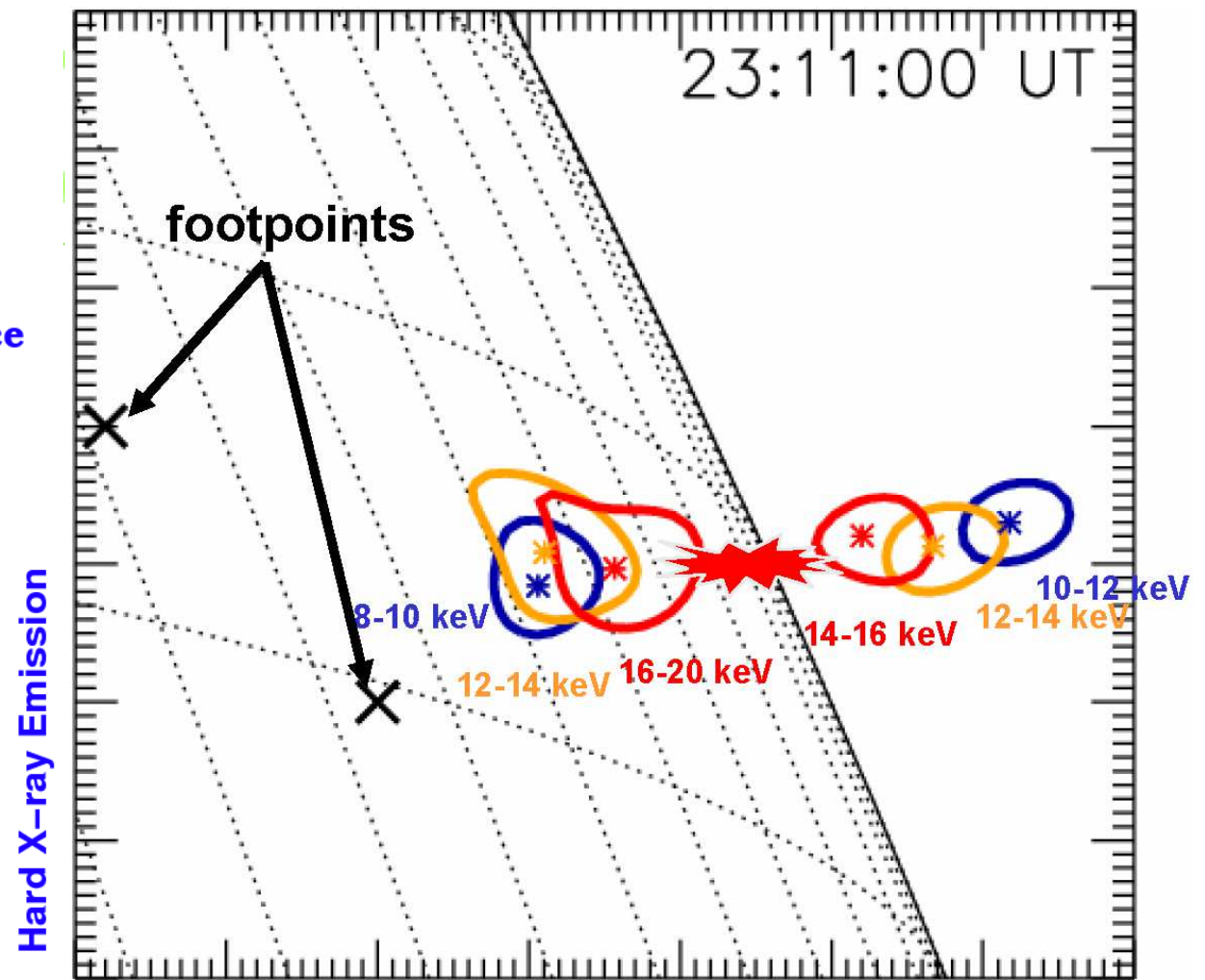


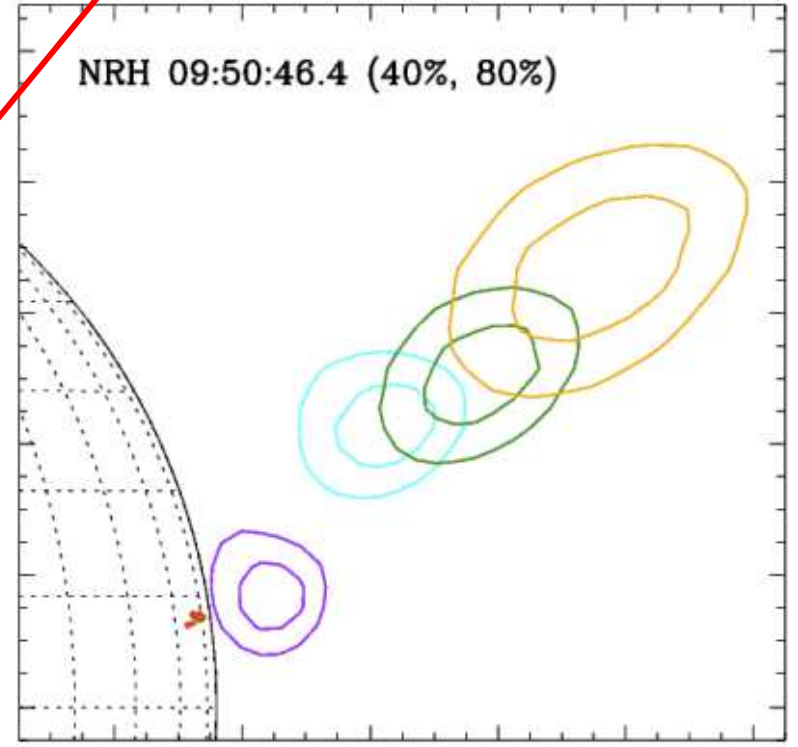
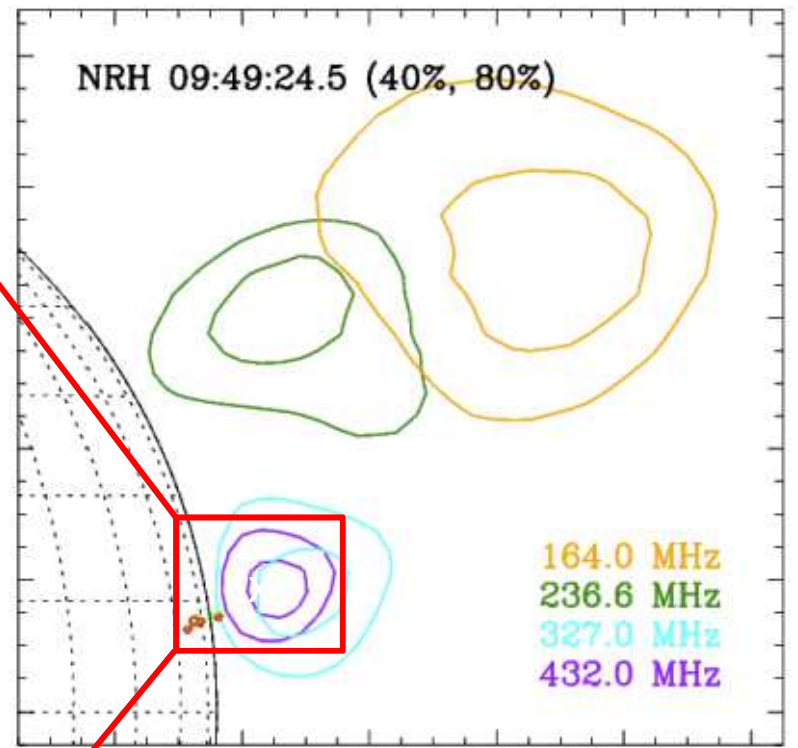
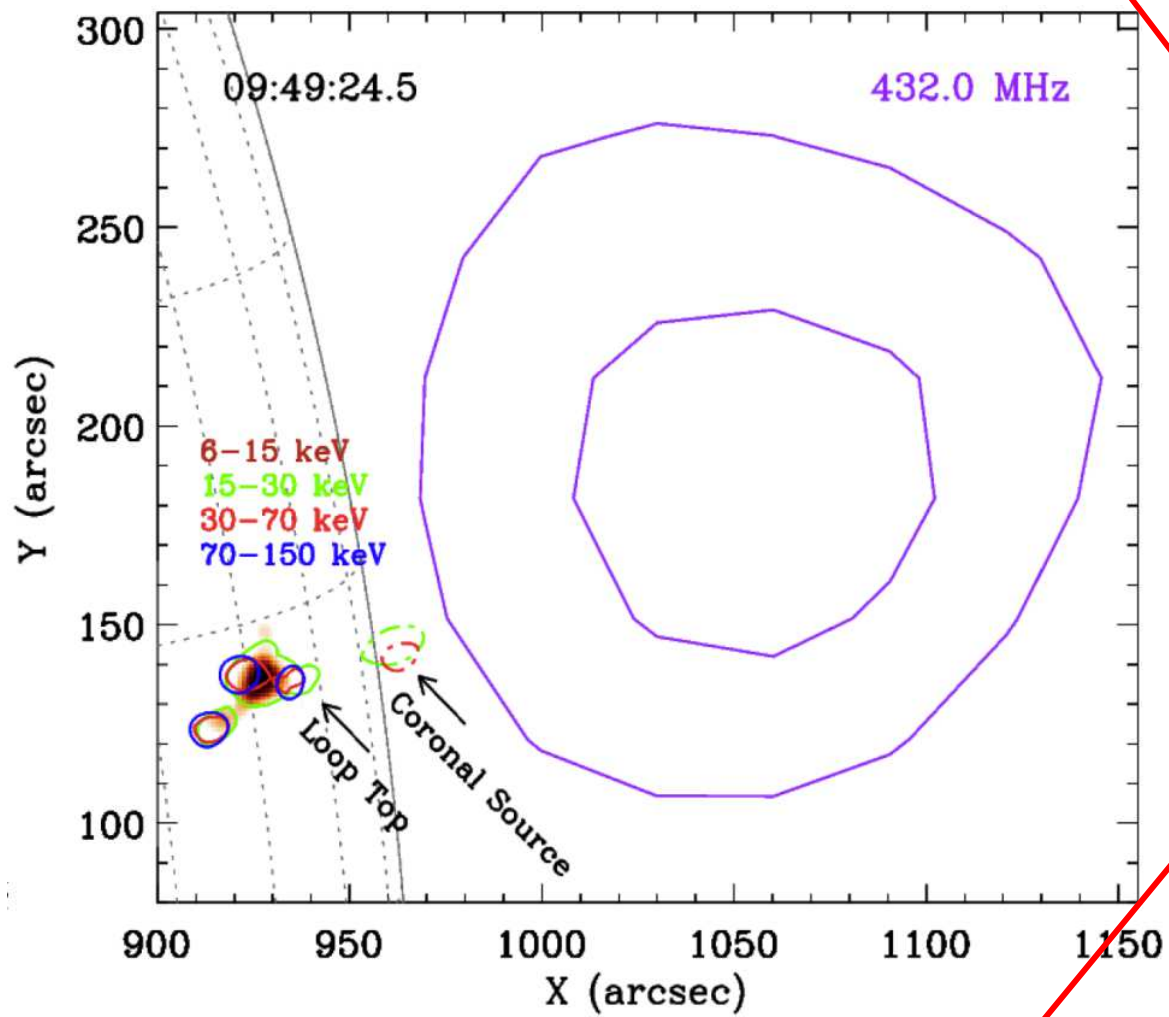
Fig. 12.14 & Fig. 12.15 in Markus J. Aschwanden (2005)

Double Coronal Sources

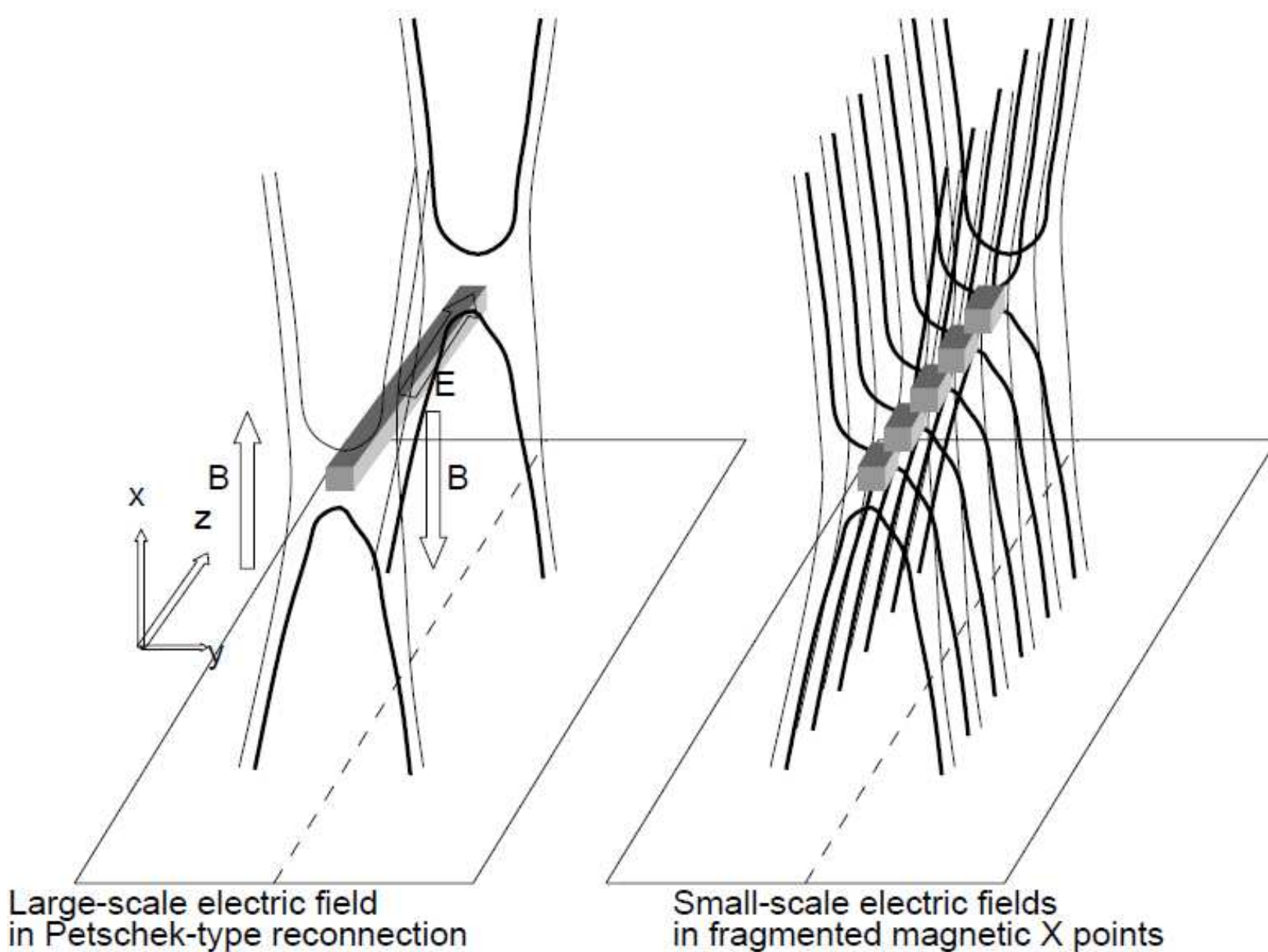


HXR coronal sources:
close to acceleration site





Electric DC-Field Acceleration



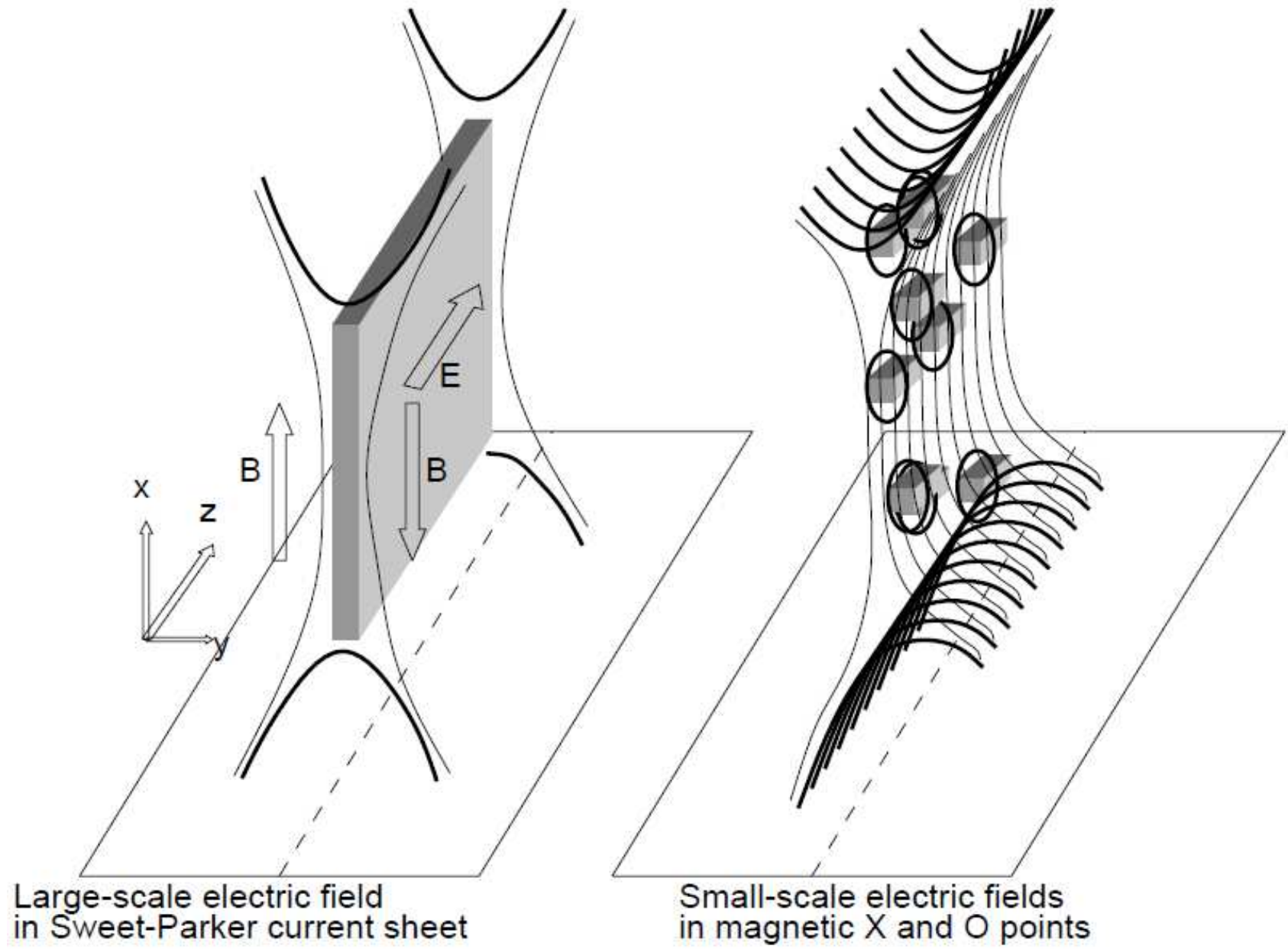
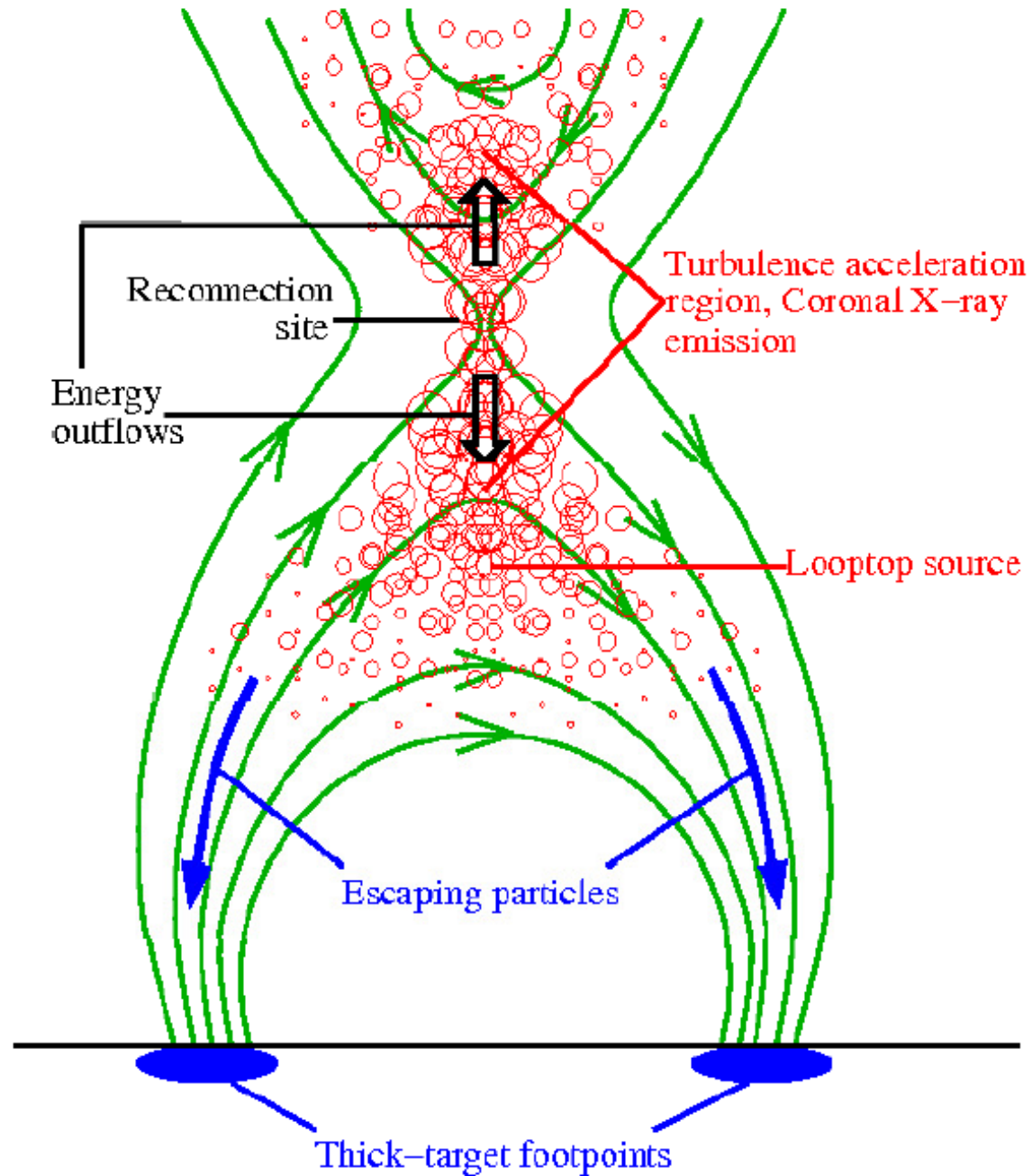
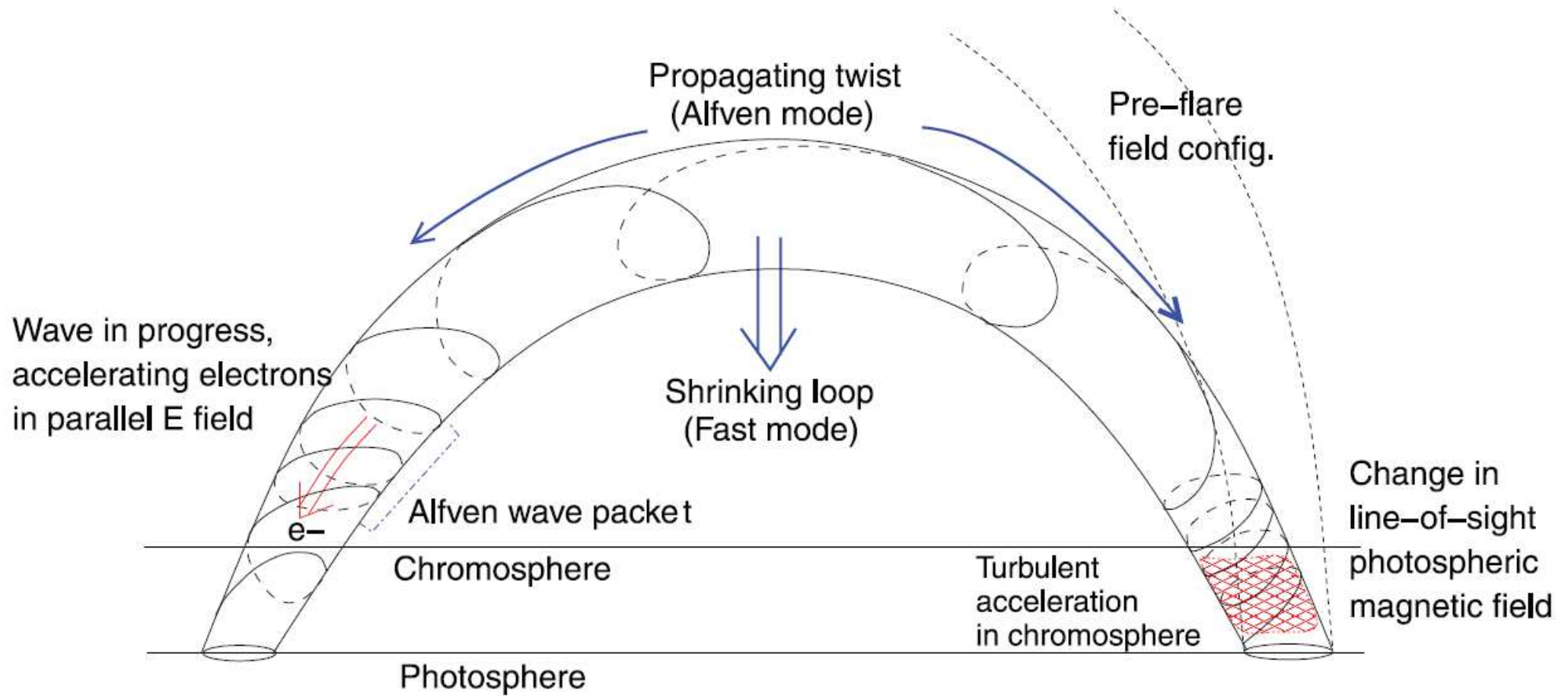


Fig. 11.2 in Markus J. Aschwanden (2005)

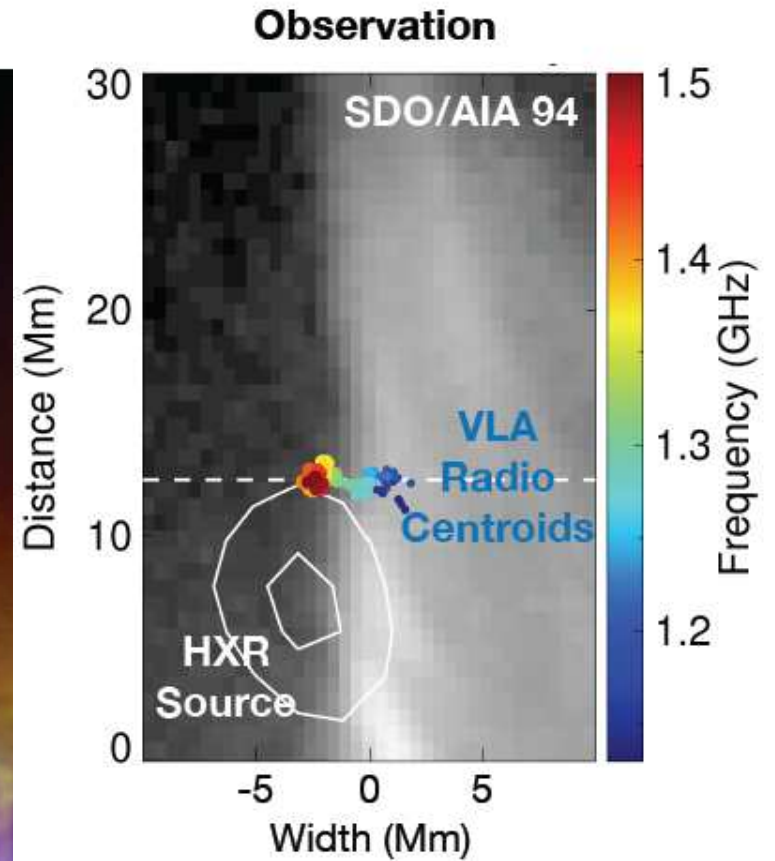
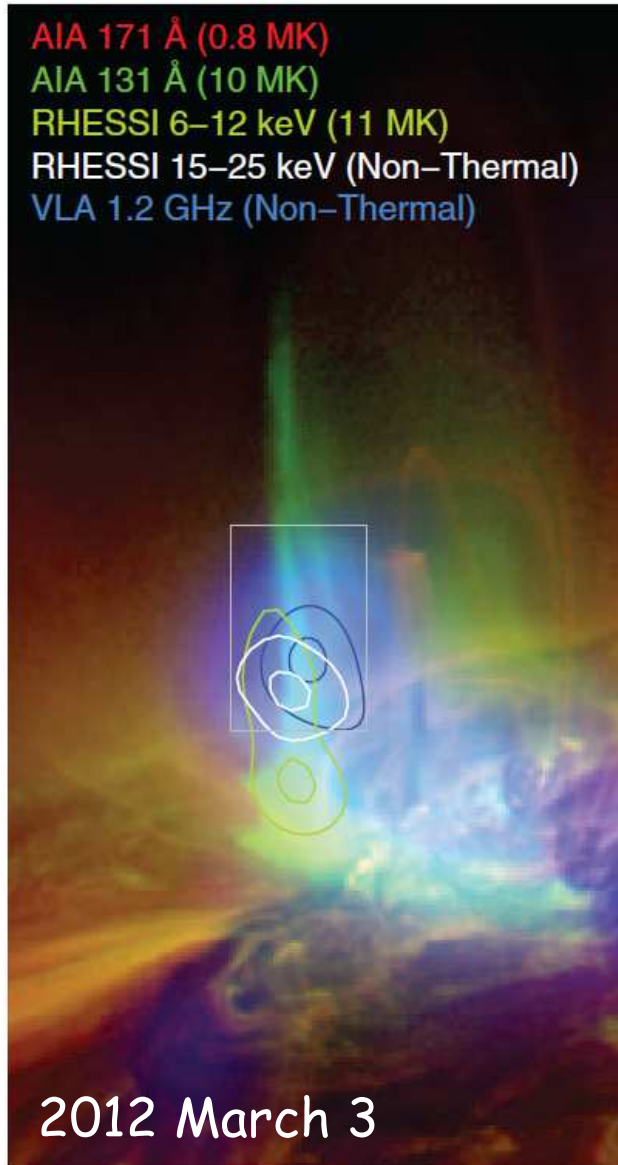
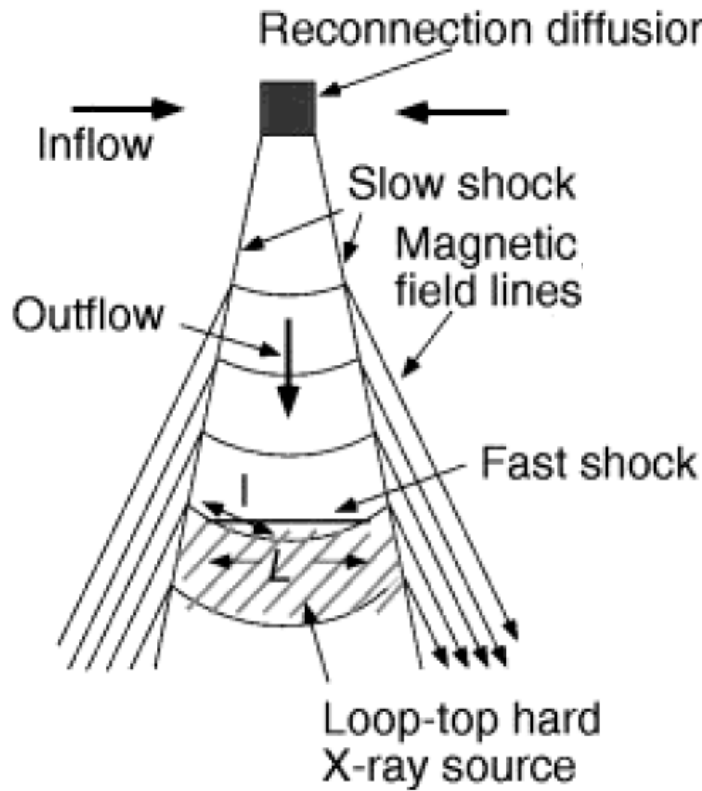
Stochastic Acceleration

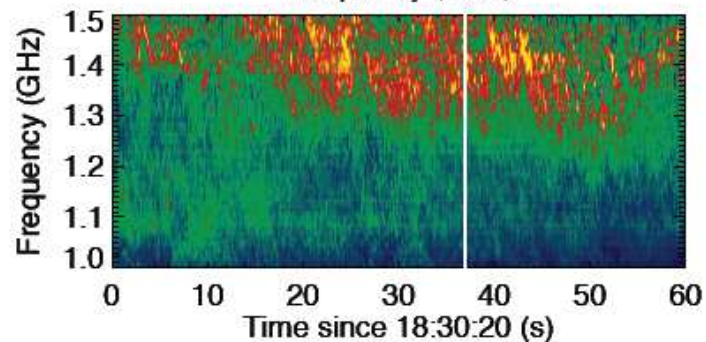
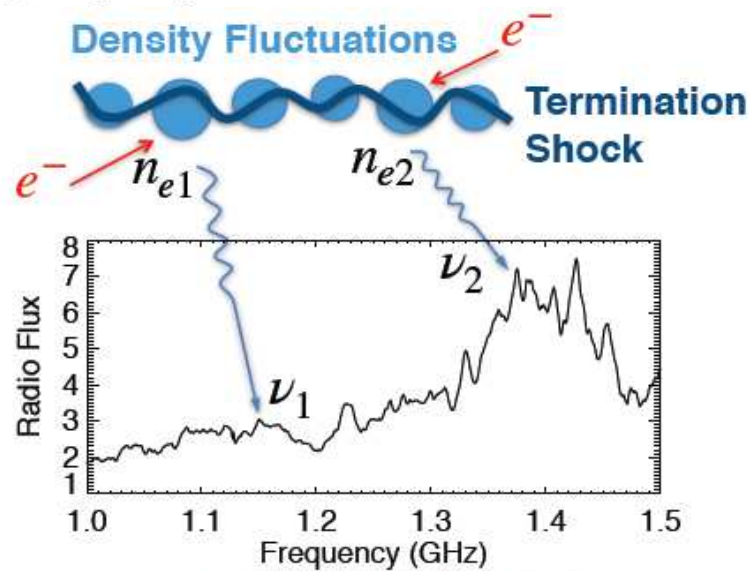
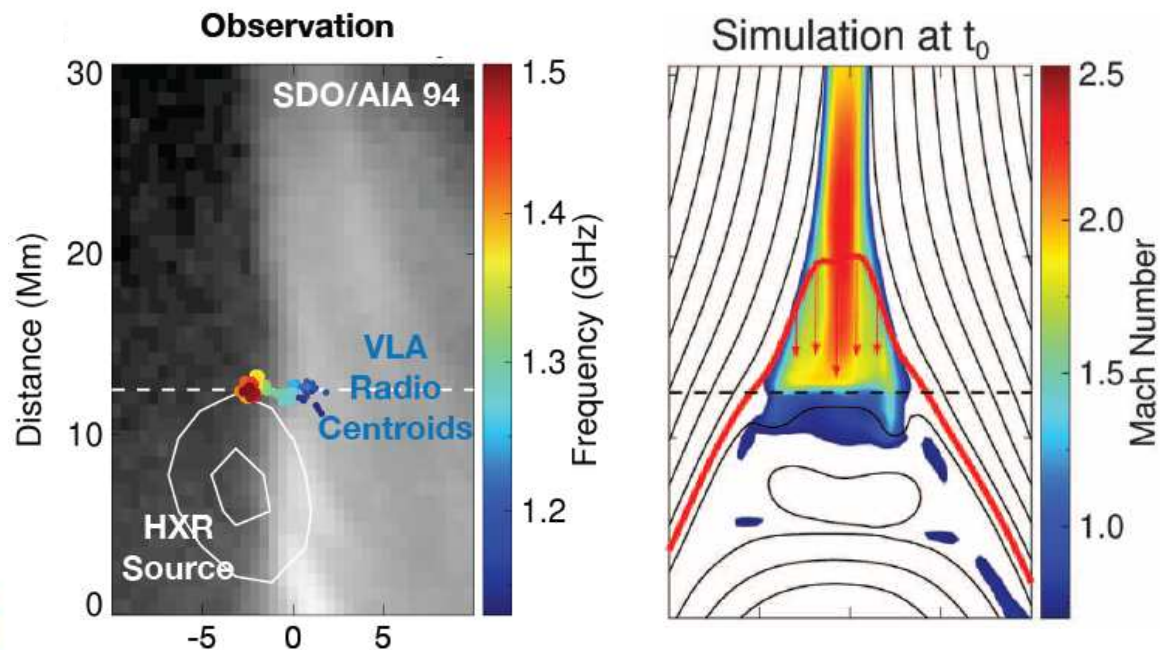
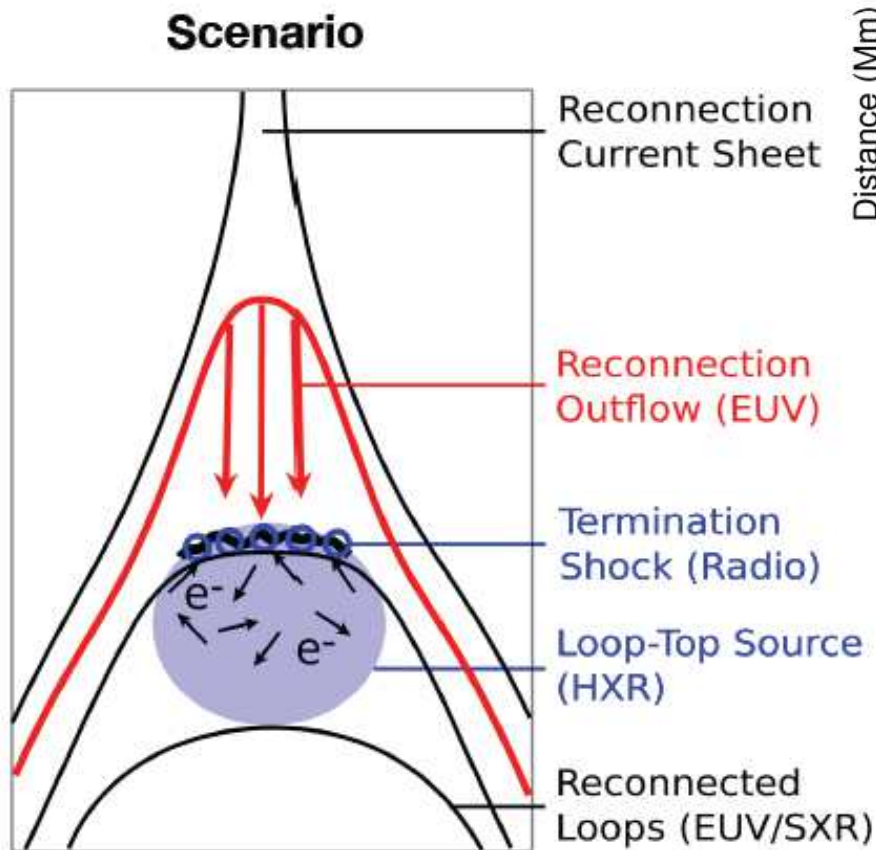


Wave-Particle Interaction

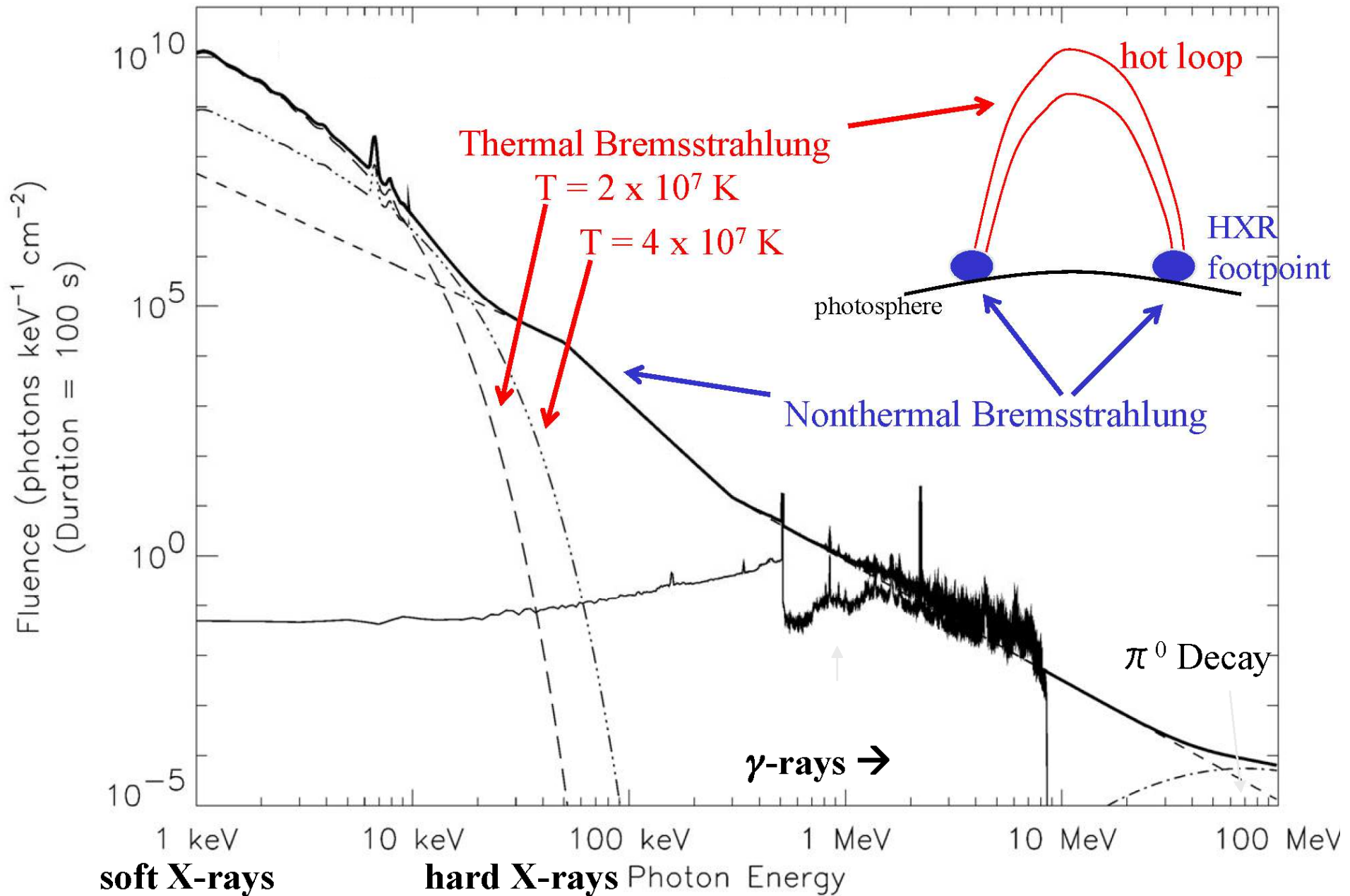


Shock Acceleration

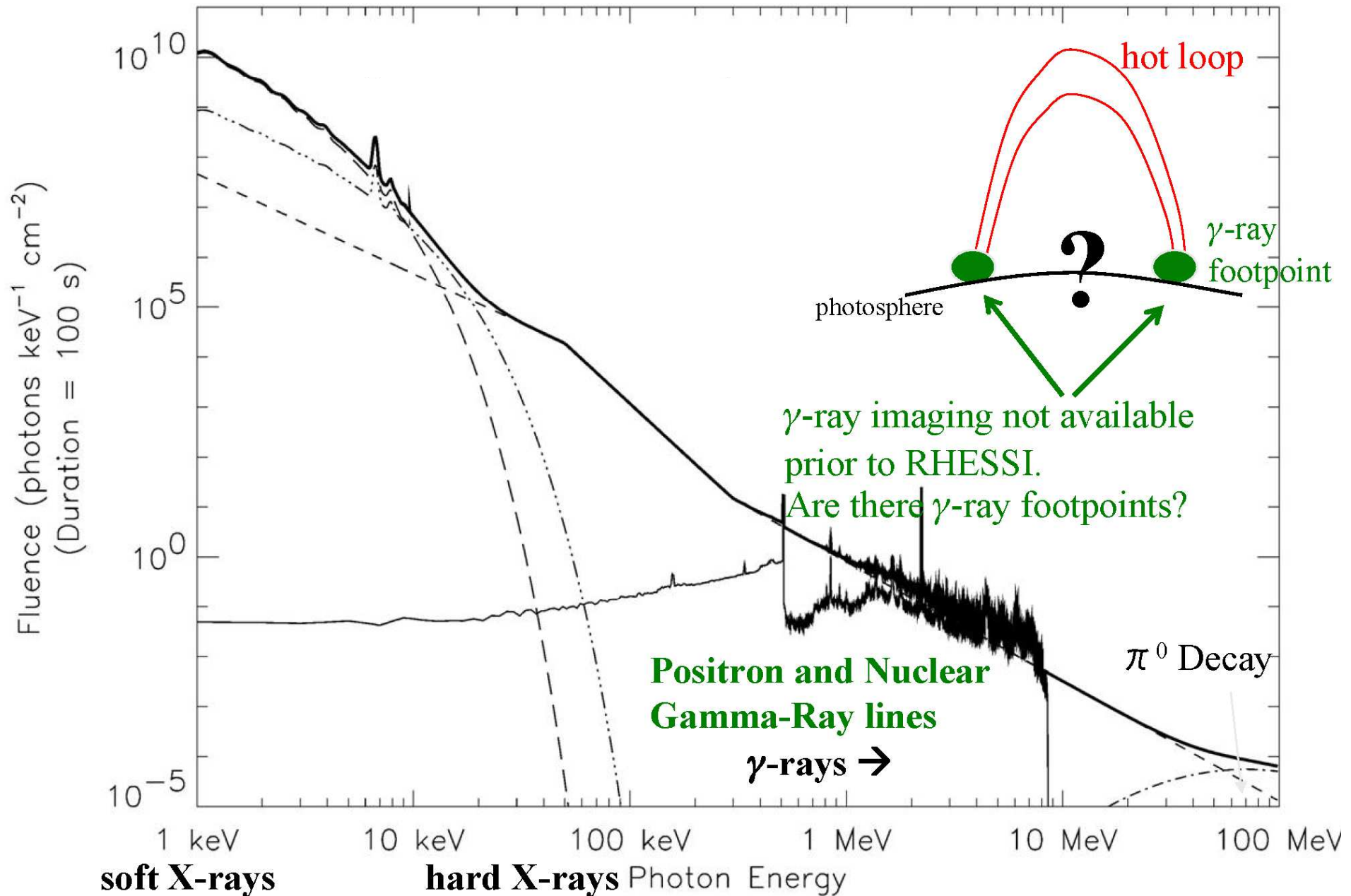




Composite Solar Flare Spectrum



Composite Solar Flare Spectrum



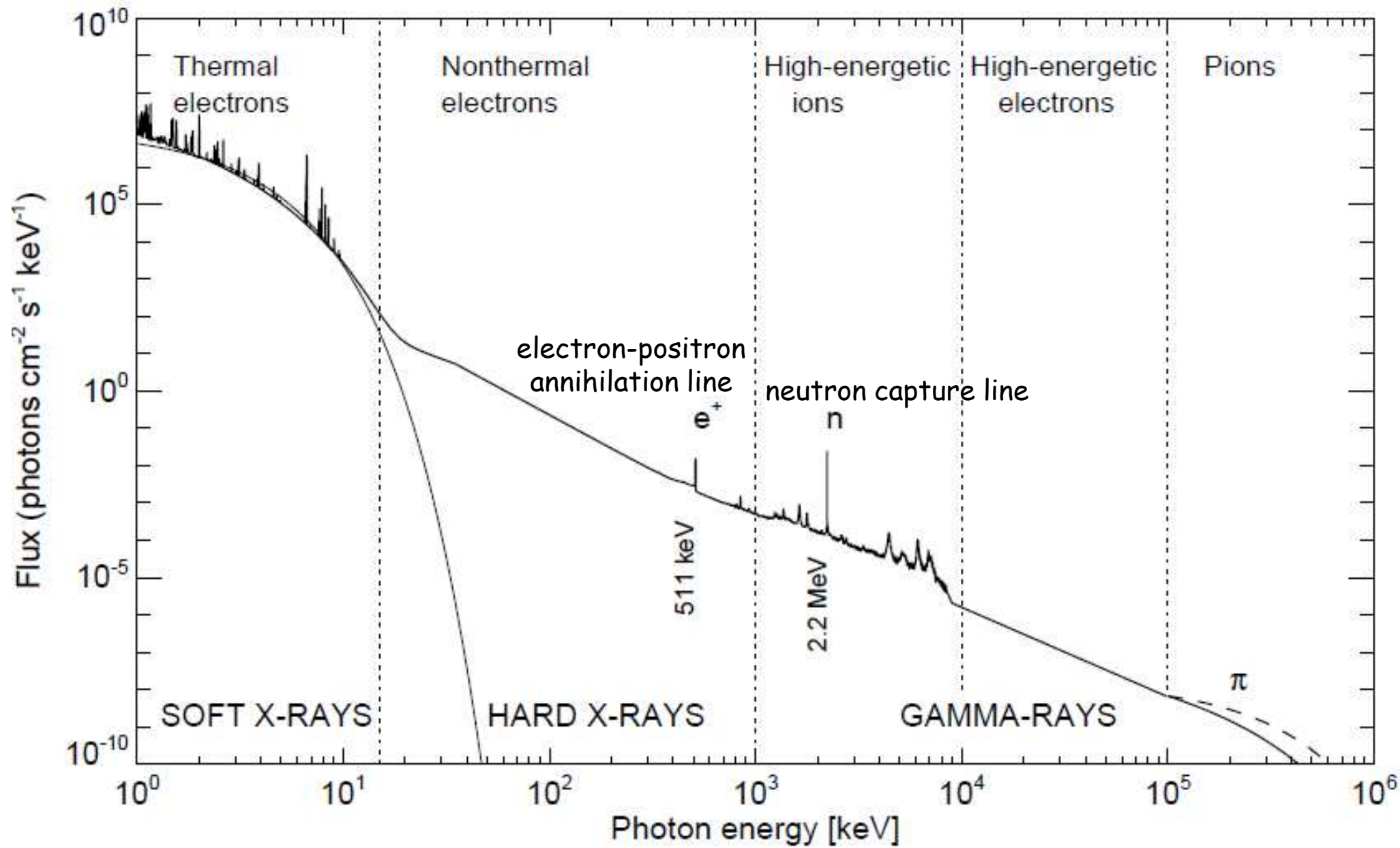


Fig. 14.1 & Fig. 14.7 in Markus J. Aschwanden (2005)

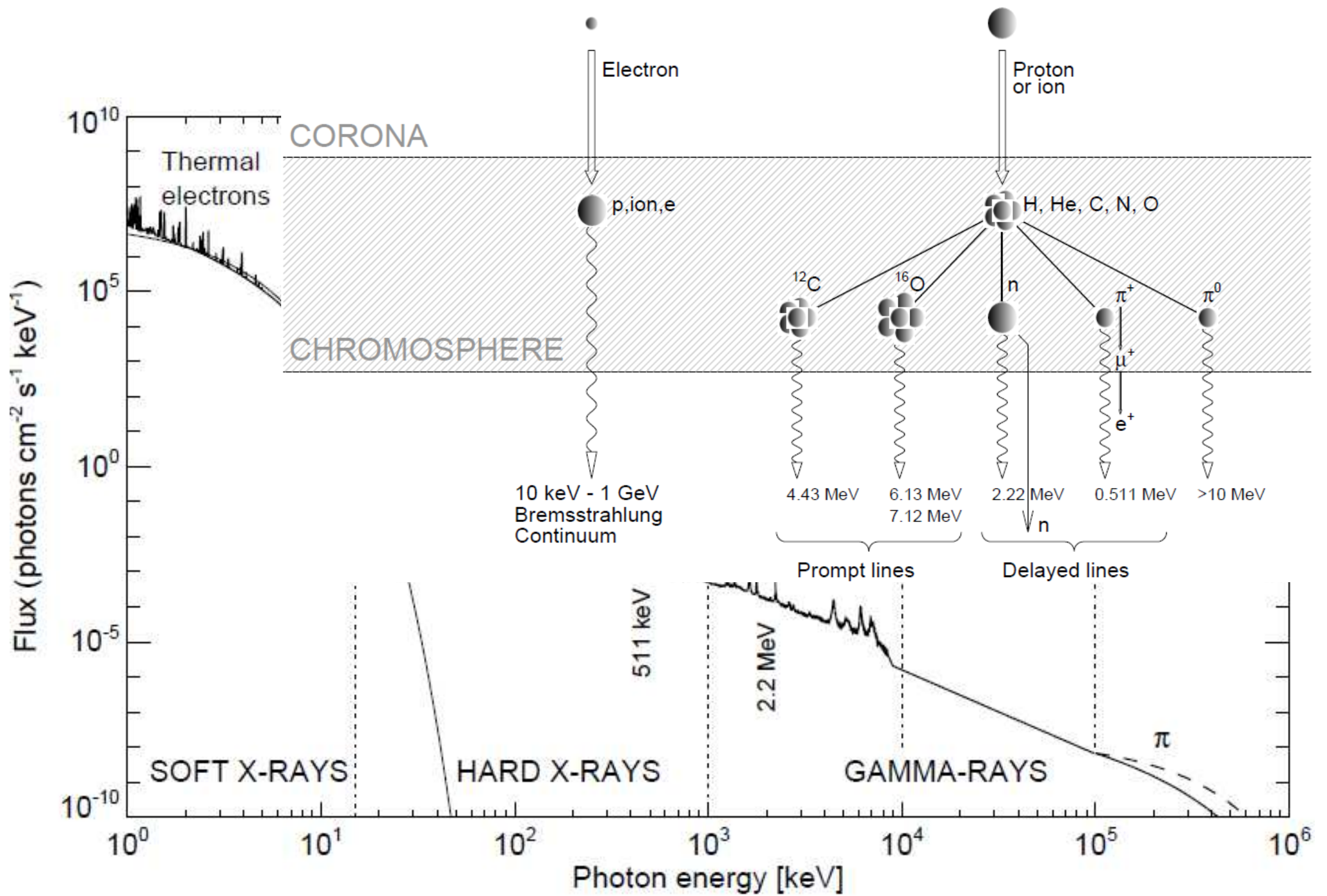
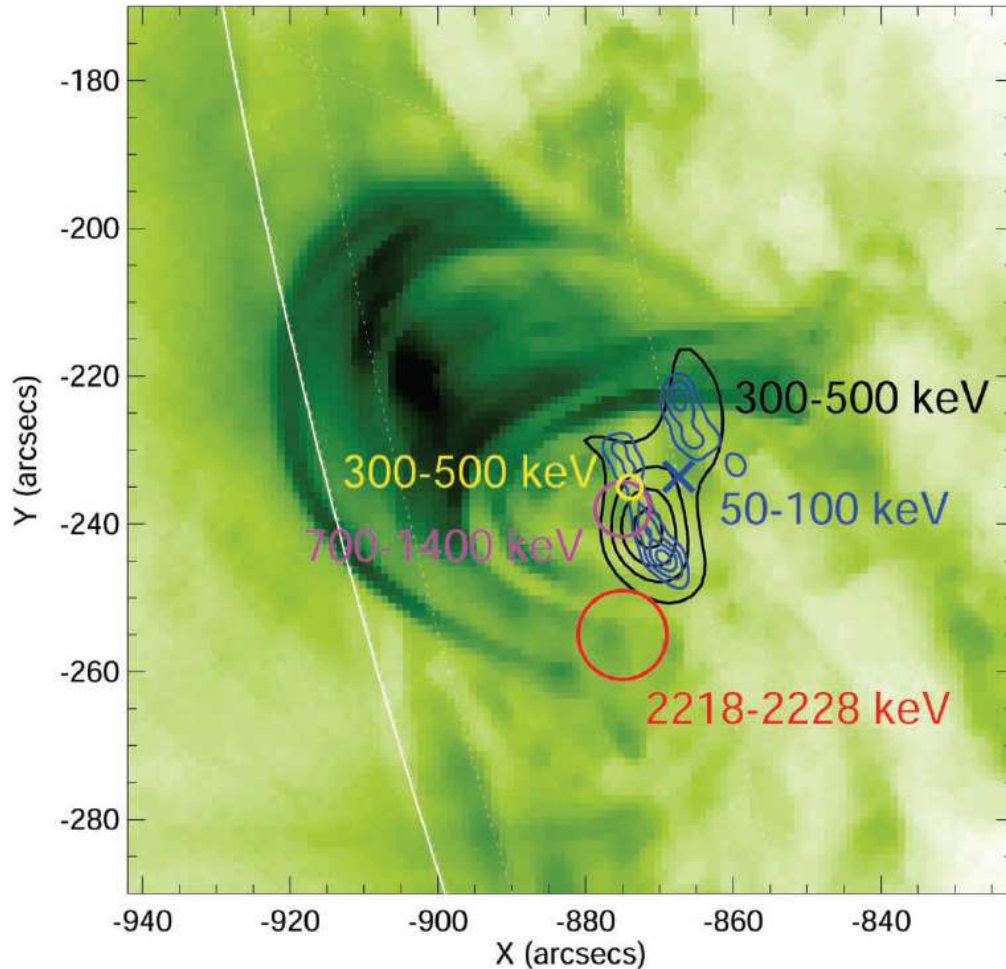
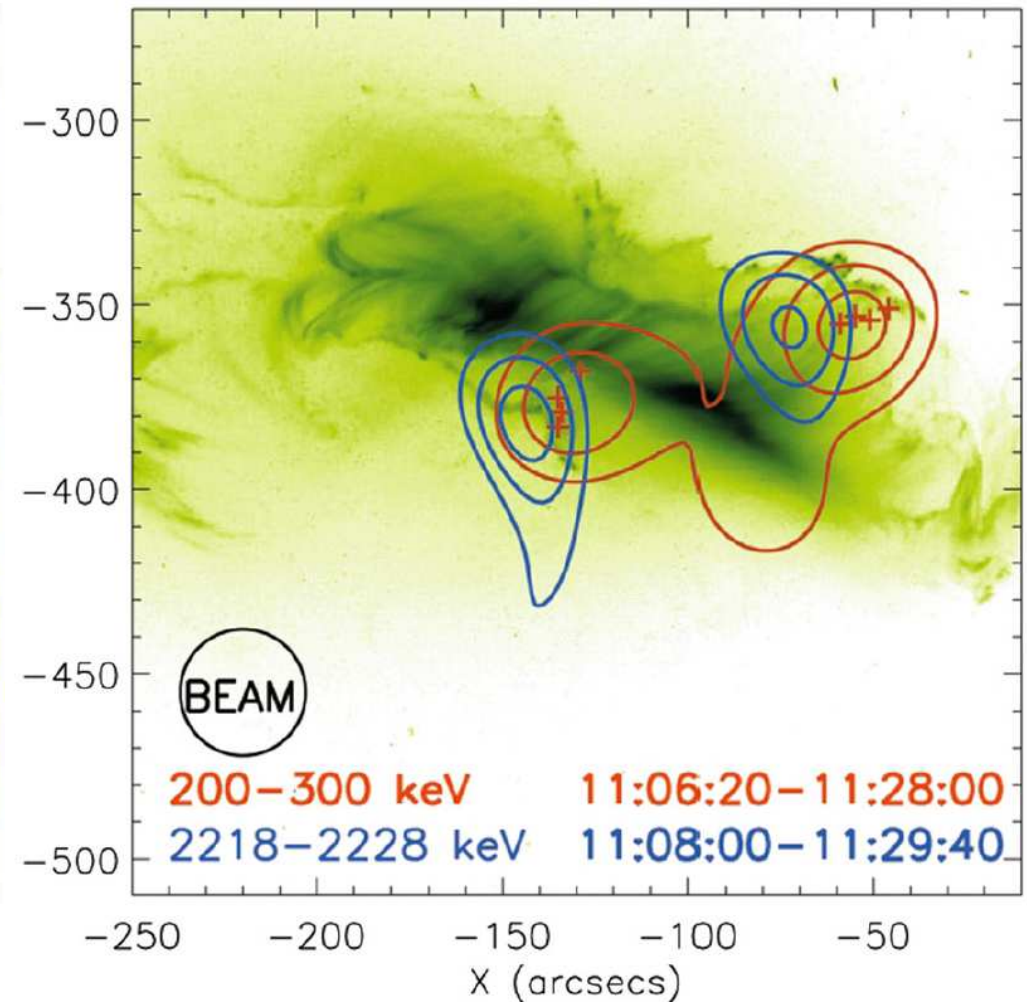


Fig. 14.1 & Fig. 14.7 in Markus J. Aschwanden (2005)

2002 July 23 X4.8



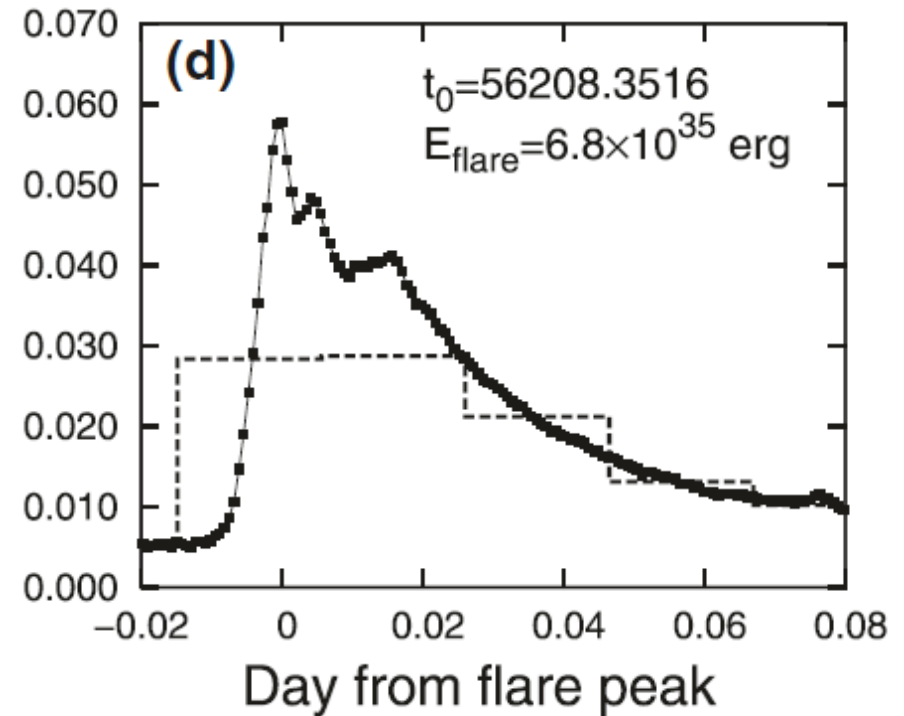
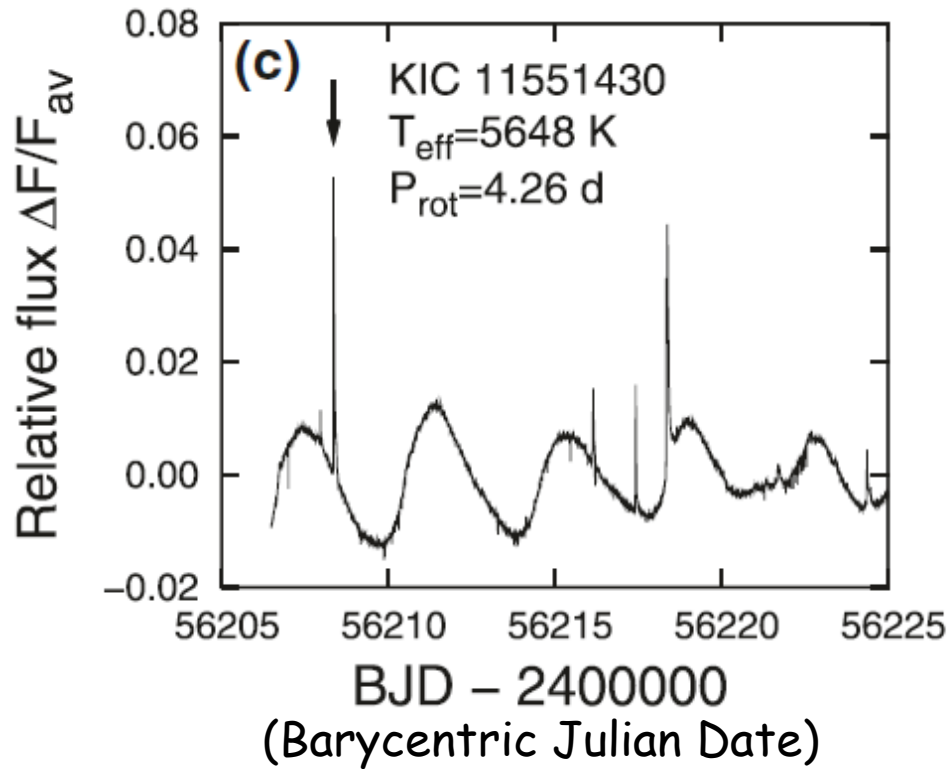
2003 October 28 X17



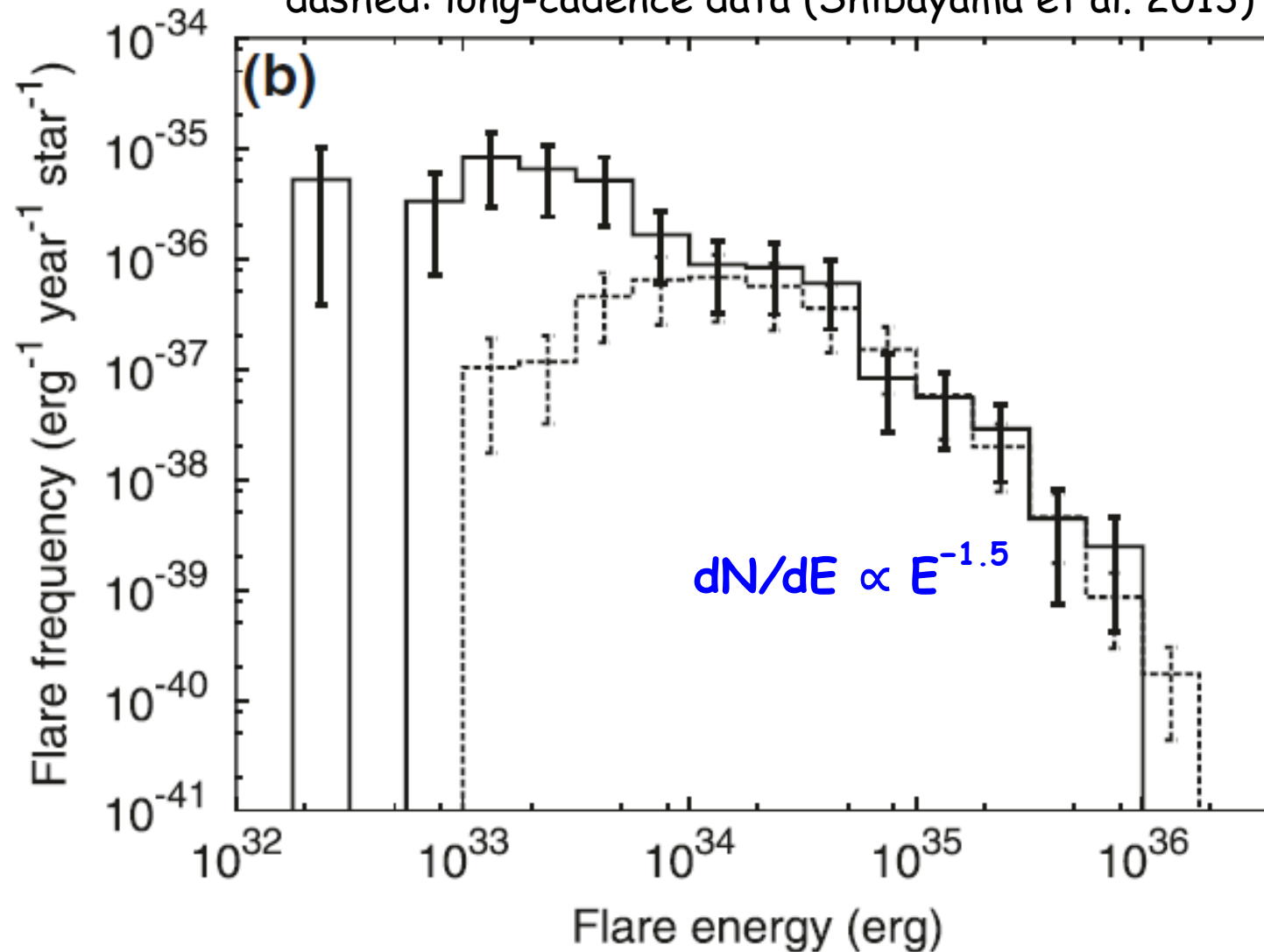
RHESSI found that the footpoints of the 2.223 MeV line— indicating ion precipitation—and the footpoints of the non-thermal continuum emission— produced by precipitating electrons—do not always coincide. This implies spatial differences in acceleration and/or propagation between the flare-accelerated ions and electrons.

Superflare

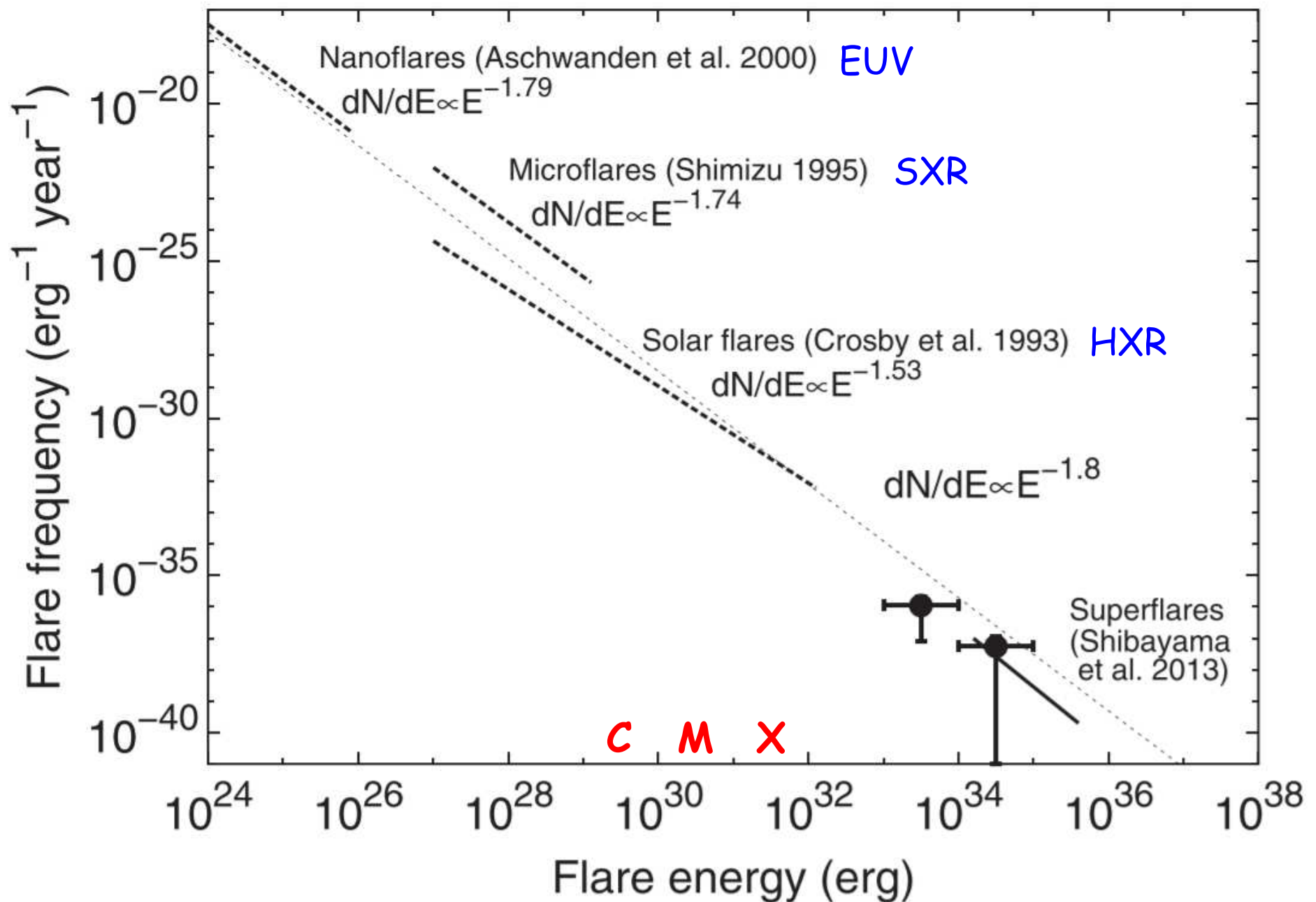
187 superflares on 23 solar-type stars with the energy ranges from the order of 10^{32} to 10^{36} erg using 1-min sampling of Kepler data



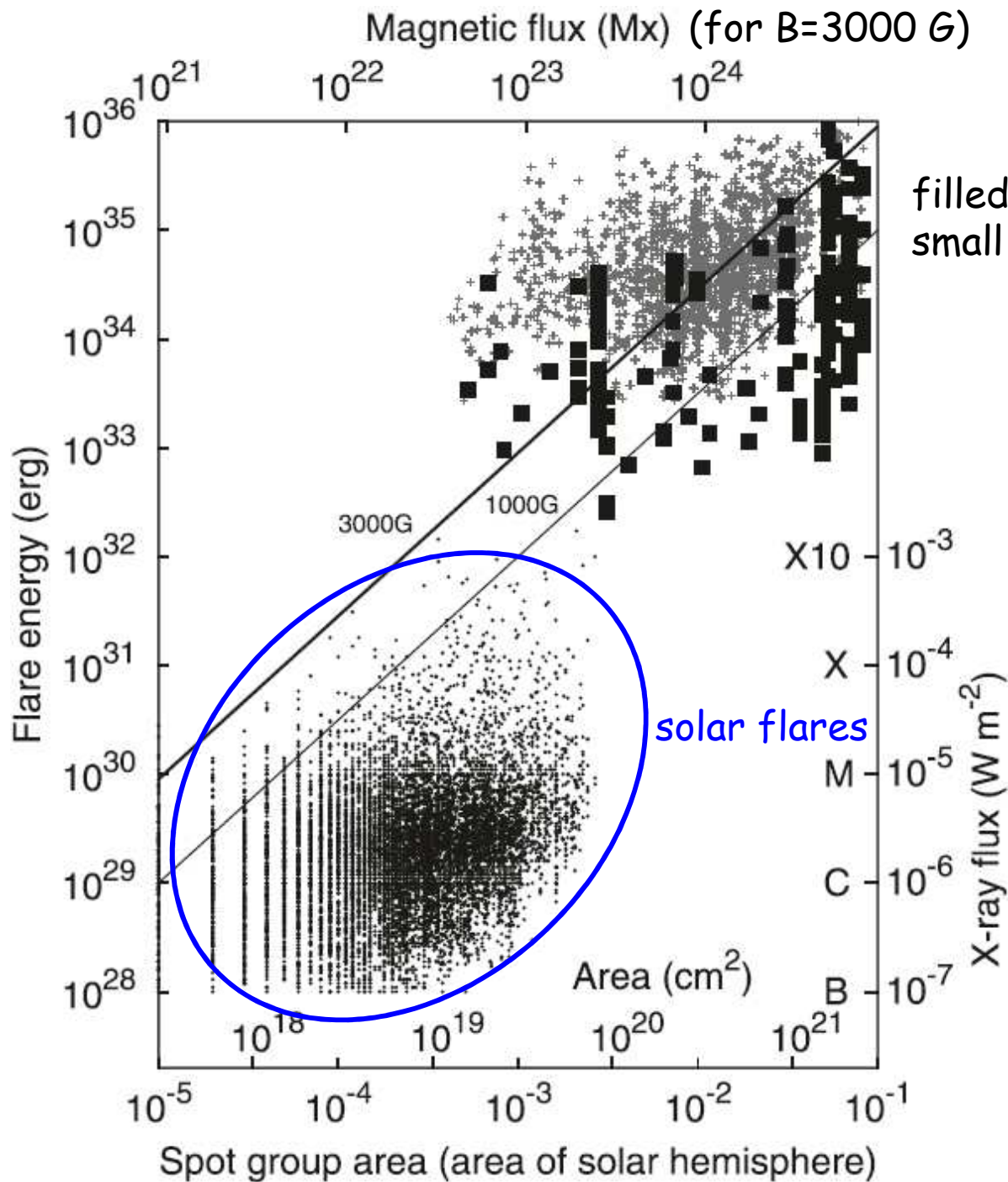
solid: short-cadence data (this work)
dashed: long-cadence data (Shibayama et al. 2013)



Using the combined data set from both short- and long-cadence data, the power-law index is -1.5 ± 0.1 for the flare energy of 4×10^{33} to 1×10^{36} erg.



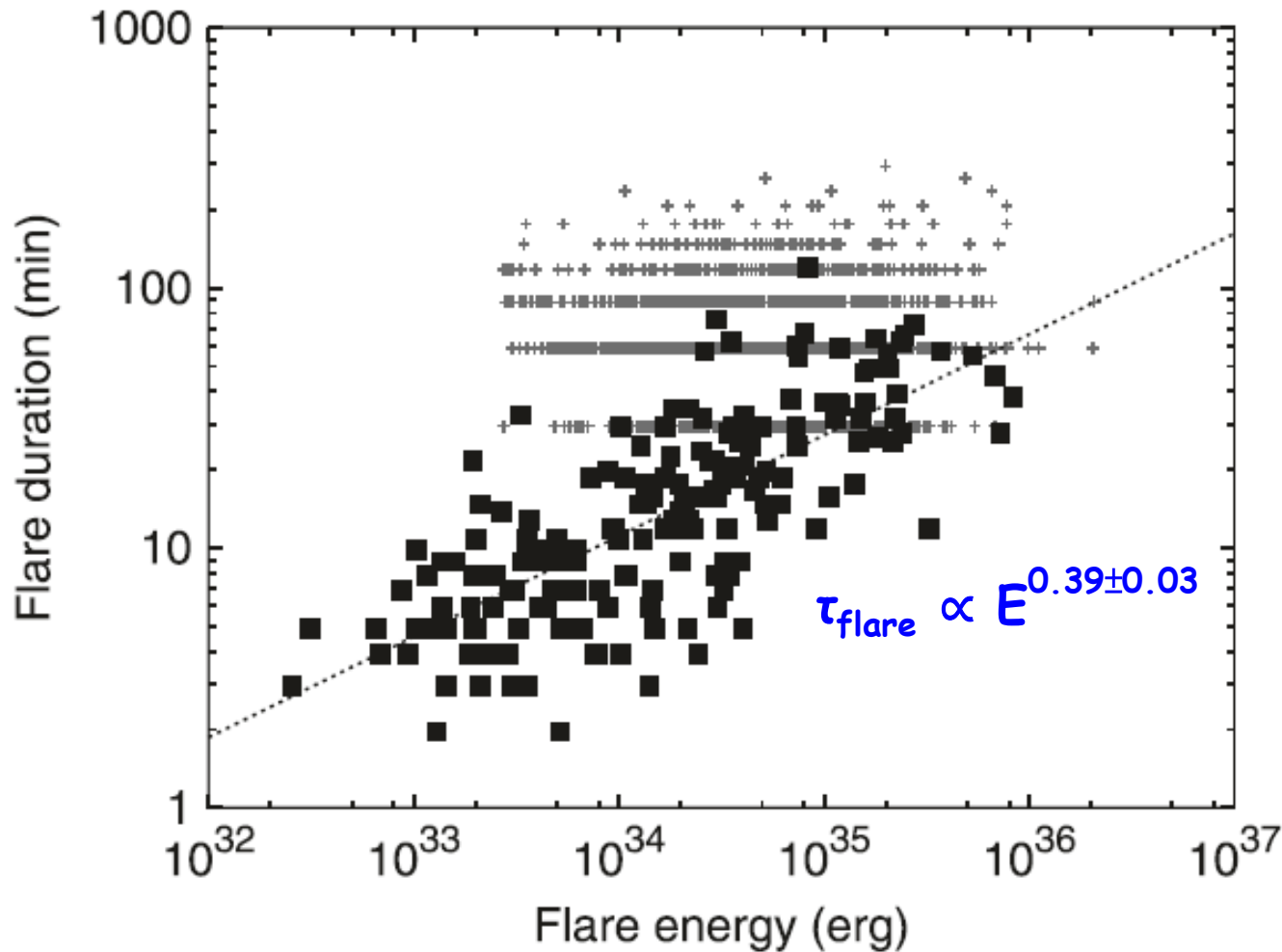
Occurrence frequency distributions of superflares on Sun-like stars and solar flares are roughly on the same power-law line with an index of -1.8 (thin solid line) for the wide energy range between 10^{24} and 10^{35} erg.



filled squares: short-cadence data
 small crosses: long-cadence data

$$E_{\text{flare}} \sim f E_{\text{mag}} \sim \frac{f B^2 A_{\text{spot}}^{3/2}}{8\pi}$$

f is the fraction of magnetic energy released by the flare. The typical value of f is in the order of 0.1.



Theoretically,

$$E_{\text{flare}} \sim fE_{\text{mag}} \propto fB^2L^3$$

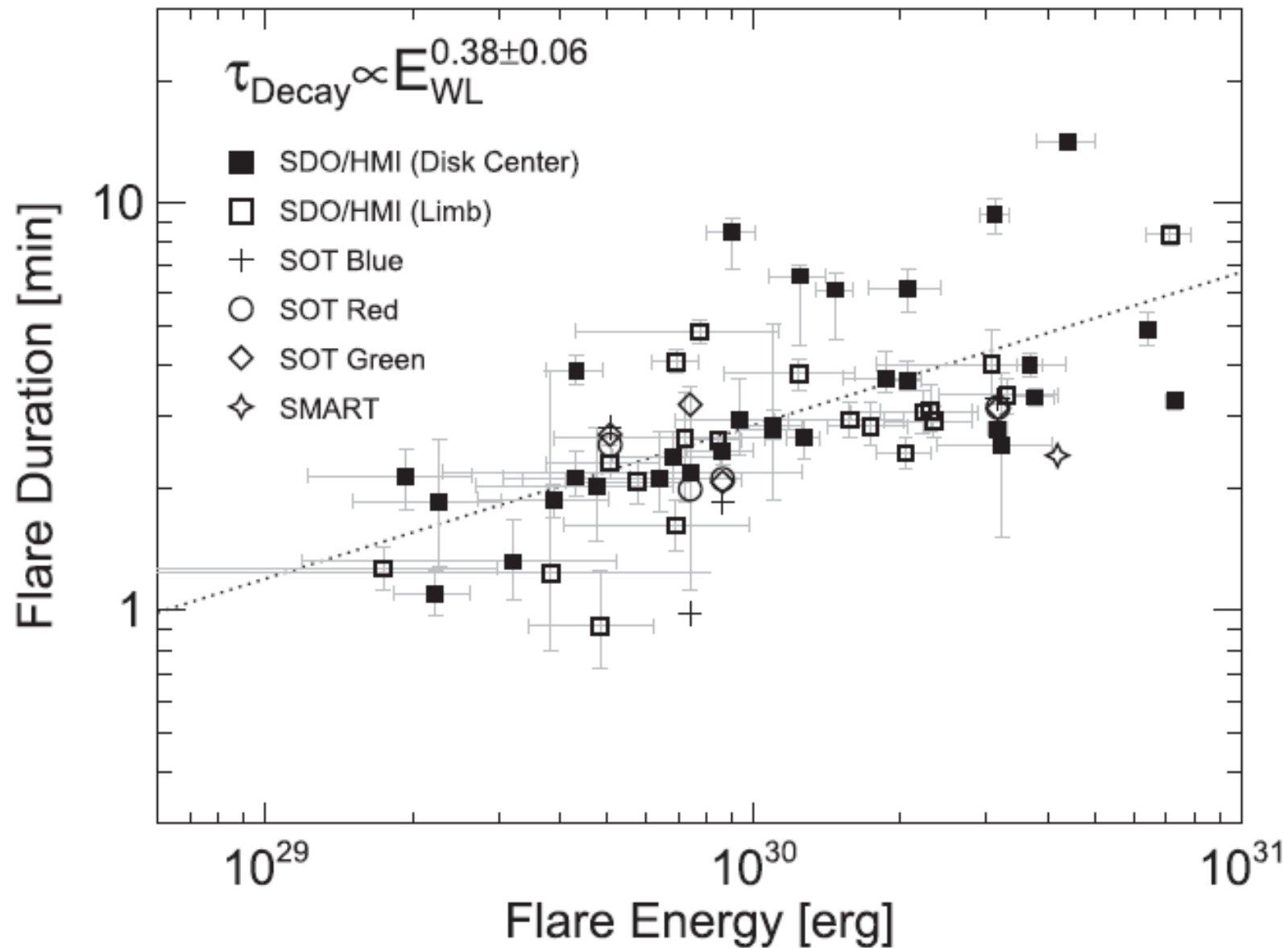
$$\tau_{\text{flare}} \sim \tau_{\text{rec}} \sim \tau_A/M_A \\ \sim L/v_A/M_A$$

τ_A is the Alfvén time
 v_A is the Alfvén velocity
 M_A is the non-dimensional reconnection rate (0.01-0.1)

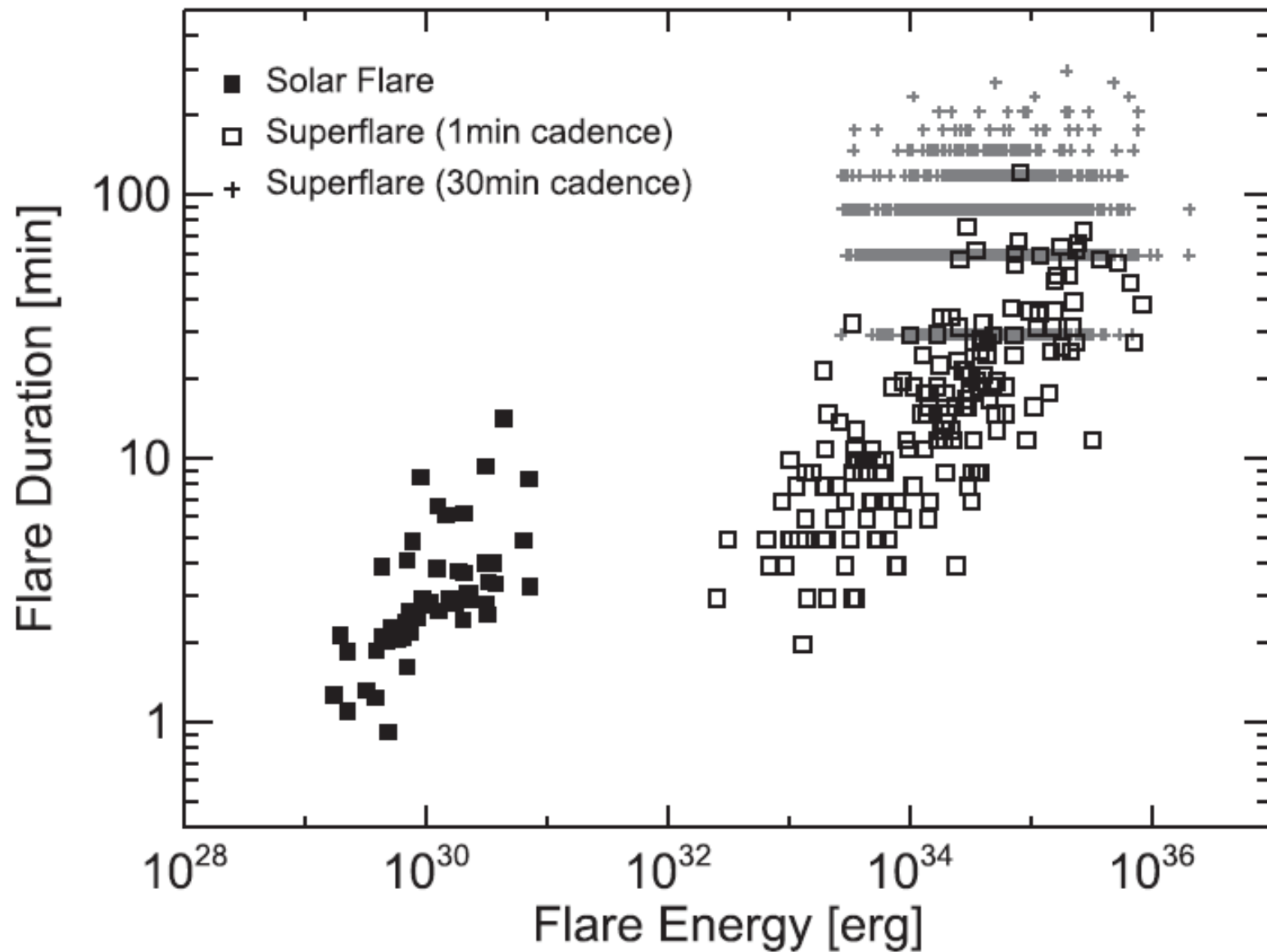
Since all *G*-type main sequence stars have similar stellar properties, B and v_A might not be so different among them. Therefore,

$$\tau_{\text{flare}} \propto E_{\text{flare}}^{1/3}$$

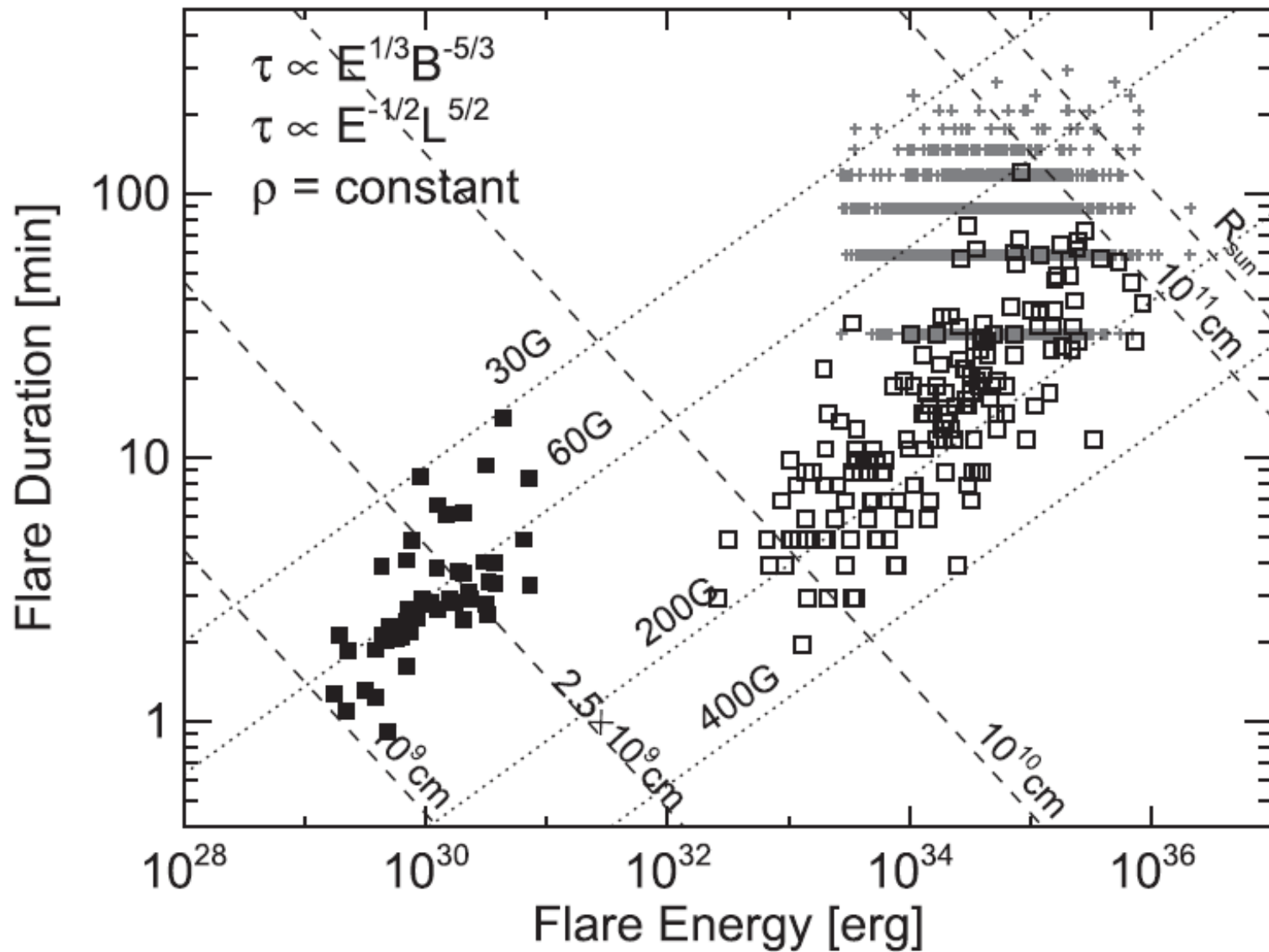
The observations show that the flare duration increases with the flare energy as $\tau_{\text{flare}} \propto E^{0.39 \pm 0.03}$.



The E- τ relation on solar white-light flares (WLFs, $\tau \propto E^{0.38}$) is quite similar to that on stellar superflares ($\tau \propto E^{0.39}$).



However, the durations of stellar superflares are one order of magnitude shorter than those extrapolated from the power-law relation of solar WLFs.



$$E \sim fE_{\text{mag}} \sim fB^2 L^3$$

$$\tau \sim \tau_{\text{rec}} \sim \tau_A / M_A \propto L / v_A / M_A$$

assuming that the pre-flare coronal density is a constant

$$\tau \propto E^{1/3} B^{-5/3}$$

$$\tau \propto E^{-1/2} L^{5/2}$$

The distribution can be understood by applying a scaling law ($\tau \propto E^{1/3} B^{-5/3}$) derived from the magnetic reconnection theory. The observed superflares are expected to have 2-4 times stronger magnetic field strength than solar flares.